Coupled Oscillation Modes of Model Ocean Wave-Energy Converters

Richard Manasseh[1], Benjamin Pocock[1], Daphne Briffa[1], Bradley Joyce[1] & Coriolan Rat[2]

[1]Department of Mechanical and Product Design Engineering,
Faculty of Science, Engineering & Technology
Swinburne University of Technology, VIC 3122, Melbourne, Australia

[2]Institut National Polytechnique ENSEEIHT, Toulouse, France

Abstract

Analytic models representing the coupling of small numbers of ocean Wave Energy Converters (WECs) are presented. The eigenmodes of collective oscillation under two conditions of coupling are explained. A simple laboratory experiment illustrates that significantly different resonance curves occur when pairs of machines are given different orientations relative to the incoming wave direction, possibly exciting different eigenmodes. The results suggest that arrays of WECs may collectively operate in a significantly different way to that expected from individual, isolated machines. This may offer potential benefits, but also potential detriments if coupled oscillation modes are not understood.

Introduction

Ocean wave-power machines or Wave Energy Converters extract renewable energy from ocean waves. They are currently under development worldwide [1]. Once individual machines are tested at full scale, more machines would be deployed in the ocean nearby, creating arrays or 'farms' with a common connection to the electricity grid. Most machines are intended to be resonators; they have a natural frequency designed to be similar to the frequency of ocean waves. When they resonate, oscillating with large amplitude, they extract maximal power from the passing waves. However, almost all designs assume the machines are isolated, not in arrays.

Unlike wind turbines, ocean wave-power machines have an exceptional ability to affect each other. This issue was first recognised during the initial surge of wave-power research in the 1970s and 80s [2, 3, 4, 5] and has recently been of renewed interest [6, 7] as developers plan arrays of multiple machines. Each machine, once excited into motion, disturbs the local sea surface and thus excites neighbouring machines to oscillate as well (coupling). In some cases, there is an engineered coupling via a common connection to shore-based generators. Although there are several theoretical and numerical studies, there appears to be no experimental data on wave-machine coupling. A recent numerical study [7] found an enhancement to the collective efficiency of the machines of over 30 % in some cases, provided the array was appropriately configured. However, inappropriate arrangement resulted in performance up to 40 % worse.

Most theoretical and numerical models of WEC dynamics assume the machines and their hydrodynamics can be represented by sets of ordinary differential equations. Some of these models incorporate nonlinear as well as linear damping terms [8], and the majority leave the co-efficients of the terms to be determined ultimately by full-scale experimentation. Nonetheless, simple ordinary differential equation models of WECs can in some cases be rigorously derived from the Navier-Stokes equations, subject to several untested assumptions [9]. Thus, irrespective of machine type, the dynamics of all WECs based on the principle of resonance are typically represented in the literature by the classical, linearly-damped oscillator, given by

$$\ddot{\xi} + 2\zeta\omega_0\dot{\xi} + \omega_0^2\xi = Fe^{i\omega t}, \tag{1}$$

where ξ is the machine's displacement, ζ its damping ratio, ω_0 its radian natural frequency, the force per unit mass exerted by waves on the machine has amplitude F and radian frequency ω, and overdots denote time derivatives. Linear damping would only be rigorously justifiable in the case of laminar flow. Full-scale WECs are large machines, many tens of metres in size. Since the flow is inherently reciprocating, there is a zero mean flow and the velocity periodically and sinusoidally returns to zero and reverses. Experiments have shown that the flow in such systems can be laminar at zero velocity, then transition to turbulence during the deceleration phase, then re-laminarise [10]. It is still unclear what damping models to use [11].

Useful power is extracted from the device by a Power Take-Off (PTO) system. Assume that the effect of the PTO is felt by the oscillator as another form of linear damping. Then the damping ratio is composed of two parts, $\zeta = \zeta_\mu + \zeta_P$, where ζ_μ is the damping ratio due to all forms of 'parasitic' mechanical loss from the system, including thermal losses, bearing friction, fluid turbulence, water-wave radiation, etc, all assumed linear; and ζ_P is the assumed-linear damping due to the PTO load, which represents the 'useful' loss from the system. A detailed description of one PTO model is presented in [11].

Now consider two WECs that are identical linear damped oscillators as in (1) but are close enough to influence each other. Clearly, the oscillations of one device would generate waves, and more generally, pressure perturbations undersea, that will excite its neighbour into motion. Furthermore, once the neighbour responds to the perturbations created by the first machine, it will in turn generate its own perturbations that will modify the behaviour of the first device, and so on, in a theoretically infinite series of reflections. This is one manifestation of the *multiple scattering* problem in physics, first studied in the context of quantum mechanics and re-considered in a number of other classical physics contexts, such as bubble acoustics [12, 13].

The issue of how to represent the influence of one device on the other has received significant attention in the WEC literature, and a number of theoretical models of coupled WECs exist, e.g. [2, 4, 5] as well as recent numerical implementations [7].

Following the normal oceangraphic conventions, both the incident ocean waves and waves emitted by the devices are assumed to be linear and inviscid. Thus the oscillatory flow in the sea is potential flow [2]. This implies that the velocity fields of the devices can be linearly superposed. For the purposes of the present paper, we represent the interaction of devices at a particular spacing by

$$\ddot{x}_1 + \gamma_{12}\ddot{x}_2(t-\tau) + 2\zeta\omega_0\dot{x}_1 + \omega_0^2 x_1 = Fe^{i\omega t},$$
$$\ddot{x}_2 + \gamma_{21}\ddot{x}_1(t-\tau) + 2\zeta\omega_0\dot{x}_2 + \omega_0^2 x_2 = Fe^{i\omega t}, \tag{2}$$

in which γ_{12} and γ_{21} represent the strength of the coupling, and τ is the time delay owing to propagation from one device to another. Furthermore, a new variable x_i has been introduced to emphasise that a self-consistent assumption has been applied [12]. This implies that all multiple scattering reflections are already taken into account, so that (2) represents a long-term steady state. While it avoids treating an infinite sum of reflections, the disadvantage of the self-consistent assumption is that the new variable x_i is no longer physically related to the physical variable ξ_i [12]. Therefore, (2) should only be used to determine eigenfrequencies and not to predict actual device displacements. The equations (2) are delay differential equations. In general, the term $\gamma_{ij}\ddot{x}_i(t-\tau)$ is itself an approximation derived from the integral over the vertical direction of the potential flow relation for a source of radially-spreading waves [2, 5], which will consist of the hyperbolic functions in the vertical from classical Airy wave theory, and Hankel functions (complex Bessel functions of the first and second kind) representing the radial structure. The exact form of this potential flow relation will depend on the boundary conditions. Since the boundary conditions are specific to each WEC type, and an analytic representation is not necessarily available, we will not detail the potential-flow relation here, but rather leave its integral representation as the arbitrary coupling co-efficient γ.

The first approximation is to assume the devices are very close, so that there is negligible propagation delay relative to an oscillation period. In most practical cases, $\gamma_{12} = \gamma_{21} \equiv \gamma$. The solution of this system will consist of two eigenmodes, the first of which can be found by defining a new variable, $x_+ = x_1 + x_2$ and adding equations (2). The result is identical to the equation of motion of a single device given by (1) with ω and ζ replaced by, say, ω_+ and ζ_+, where

$$\omega_+ = \frac{\omega}{\sqrt{1+\gamma}},$$
$$\zeta_+ = \frac{\zeta}{\sqrt{1+\gamma}}. \tag{3}$$

This first eigenmode is usually called the symmetric mode and represents the two devices oscillating in phase. In general, the symmetric mode has a lower frequency and lower damping than an isolated device. Meanwhile, the second, antisymmetric mode is

$$\omega_- = \frac{\omega}{\sqrt{1-\gamma}},$$
$$\zeta_- = \frac{\zeta}{\sqrt{1-\gamma}}. \tag{4}$$

If devices could perform in the symmetric mode, they would collectively operate at a lower frequency. This implies that to match a given incident ocean wave frequency, a group of devices arranged to resonate in symmetric mode could have individual natural frequencies ω_0 higher than that needed for an isolated machine to resonate. Since the natural frequency is generally inversely related to the size of a machine, this implies machines could be smaller than if they had to operate in isolation, with attendant savings in manufacture and installation. Furthermore, the lower damping may imply higher useful power. However, once the time delay τ is considered, there are no simple relationships such as (3) and (4), though for small τ, approximations to these two modes will exist.

The type of WEC tested in the present paper is an OWC. Derivation of the approximate natural frequency of an OWC from first principles is straightforward, albeit based on a long chain of assumptions detailed by [9]; as a first approximation, the natural frequency is given by

$$f_0 = \omega_0/(2\pi) = \sqrt{(g/L)}/(2\pi), \tag{5}$$
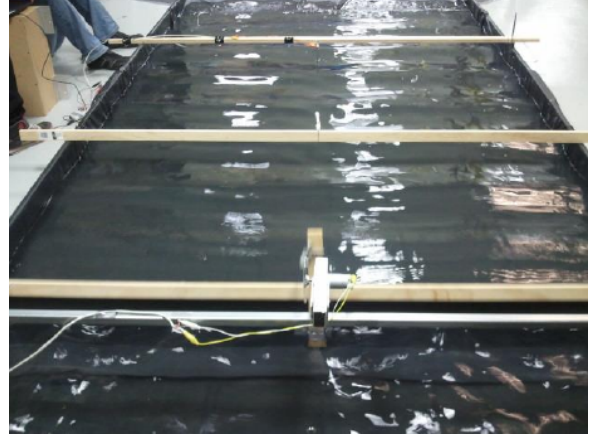
Figure 1: Wave pond showing two beams for mounting WEC models. Wavemaker assembly is in foreground.
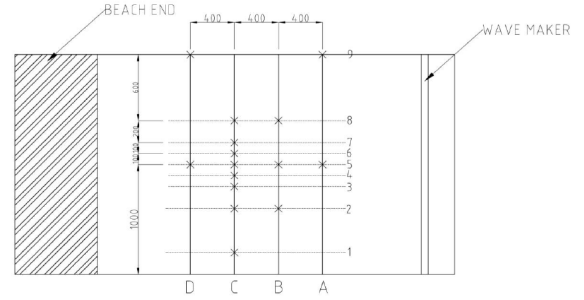
Figure 2: Wave pond geometry (dimensions in mm) showing locations of model WECs. Incident wavelength is approximately 410 mm.

where L is the length of the 'tube' of the OWC that is submerged.

Experimental set-up

Illustrative experiments were set up in a 'wave pond' designed for waves intermediate between the shallow- and deep-water approximations. The pond was a shallow rectangular pool of water 4 m long and 2 m wide and with a maximum depth of 0.15 m (figure 1). The pond walls were a timber frame laid on a concrete floor. The walls and floor were lined with 0.5 mm thick PVC swimming-pool sheeting.

The design wave height was 0.02 m peak-to-trough. A paddle-type wave maker spanned one of the 2 m wide ends of the tank. It was hinged at the pond floor. The paddle was made of core flute with a treated timber perimeter, giving both rigidity and light weight. The motor drove the paddle via a crank with a horizontal amplitude of 0.01 m at the water surface at a fixed frequency (noted below).

A wedge-shaped beach 0.75 m long at the end opposite to the wave-maker effectively eliminated reflections. The pond layout showing co-ordinates where model WECs were placed is shown in figure 2.

The wave pond was filled to a depth of 0.110 ± 0.001 m. A submersible video camera (GoPro Hero 3, 120 frame s^{-1}) imaged waves passing a ruler located at C5 on figure 2 with an accuracy of ± 1 mm within 95% statistical confidence limits. The camera data were cross-checked against a capacitance-

type wave-height sensor made in-house. Though less accurate, the camera technique was found to be more useful for making measurements of water displacement within model WECs. Waves were generated over 60 wave cycles in order to generate statistics on the incident wave quality in terms of wave height and frequency. The fixed frequency was determined to be $1.88 \pm 0.01 \text{ s}^{-1}$ within 95% confidence limits and the resulting wavelength according to classical Airy wave theory for water of intermediate depth was 0.410 ± 0.002 m, which was consistent with observation.

These tests determined that at the design frequency, waves were periodic with straight crests and that there were no observable reflections from the side walls or the beach. Nonetheless, it must be emphasised that the performance of the wave pond was neither perfect nor rigorously calibrated. For example, small kinks in the PVC sheeting forming the floor were present owing to the way this product was originally folded, and thus the depth suffered from perturbations of a few mm or a few percent. Moreover, paddle-type wave-makers cannot perfectly reproduce the underwater velocity profile of free-surface waves, and will thus create a variety of other wavelengths in addition to the intended wavelength. Hence, a rule-of-thumb in the wave-maker community is to only make measurements more than 10 wavelengths from the paddle so that undesired wavelengths have time to disperse. This was not possible since the entire pond was only 10 wavelengths long. That is why the present preliminary study is best classed as 'illustrative' rather than providing universal data. Furthermore, recalling the issue about reciprocating turbulence canvassed above and the uncertainty of scaling such systems, the flows generated in the devices were not guaranteed to represent the full scale.

Model WEC devices were designed to have a scale less than 1/10 of the incident wavelength, and thus to be consistent with the concept of 'point absorbers'. As noted earlier, our model WECs were OWCs. This type of WEC was chosen owing to the simplicity of the OWC concept: no moving parts were required in order to create a resonator. To test alternative WEC concepts at such a small scale would have required problematic parameter matching. For example, heaving-buoy type devices would have required matching of the size and buoyancy of small floats and the stiffness of small springs to give devices able to resonate in such shallow depths, a matching that proved impractical.

Since the incident waves had a 0.41 m wavelength, model OWC devices were made 0.04 m in diameter. They were made of clear acrylic tubing to enable visualisation of the water displacement inside each model device. They were fixed with adjustable collars to mounting beams spanning the pond width. As just noted, the wave-maker produced a fixed frequency. Since the natural frequency of an OWC is determined by the depth of the tube that is submerged, the adjustable collars permitted the OWCs to be tuned to the wavemaker frequency by altering their submerged depth. The video camera was again used to measure water displacements inside the models; here, however, the accuracy decreased from ± 1 mm to ± 2.5 mm owing to the poorer accuracy with which lines could be ruled on the models.

To allow initial transients to die away, measurements did not commence until 10 wave periods had elapsed. Statistics on the behaviour of model OWCs were generated by measuring the water displacement inside the devices over 40 periods. A second set of 40 data points was collected and the statistics pooled.

Results

A single device was set up and its submerged depth L varied to determine its actual resonance. As shown in figure 3 (solid line), the length L giving resonance was found to be 0.065 m. For the input frequency of 1.88 s^{-1}, the simple linear inviscid 'pendulum mode' natural frequency given by (5) requires $L = 0.070$ m for an inviscid resonance. Since from (5) $L = 0.065$ m would correspond to a inviscid natural frequency of $f_0 = 1.96 \text{ s}^{-1}$, the measured resonant frequency is lower, which is consistent with the usual influence of damping on any linear oscillator. By fitting the data to the frequency response for a classical damped oscillator, the damping ratio due to viscous losses under linear theory, δ_P, can be roughly estimated to be 0.24.

Waves in the lee of a single device had no measurable reduction of amplitude within experimental error. Since the device diameters are 1/10 of the wavelength, normal principles of wave theory suggest minimal reflection or interference of waves if the devices were solid bodies rather than resonators. As a test, the single OWC was also sealed at the bottom so that it was in practice a solid cylinder with no ability to absorb power; its only influence would then be to scatter waves by reflection. In this case, again there was no discernable reduction of waves in the lee of the device.

An array of six devices was then set up in two rows at coordinates B and C, 8, 5 and 2 shown in figure 2. Overall, the result was a reduction in measured peak-to-peak amplitude by roughly 25-35% within the experimental error. This test confirmed the array did have a significant influence on the wave height, though the test did not assess if the reduction in wave amplitude was due to enhanced displacement of the devices in the array, which would represent useful power extraction, or to scattering of waves, which would be a loss.

A pair of devices was then set up to determine if there was significant coupling between devices and, if so, to measure it in detail. Two orientations were investigated. Devices were set up 0.2 m apart with the line connecting their centres parallel to wave crests (locations C4 and C6 in figure 2). This orientation was thought suitable to excite the symmetric mode, which from (3) was expected to have a lower frequency and damping than the single device, recalling that (3) is not expected to quantitatively predict the behaviour owing to the time delay.

The pair of devices was also set up 0.2 m apart and perpendicular to wave crests (locations B5 and C5 in figure 2). This orientation was thought suitable to excite the antisymmetric mode.

The half-wavelength spacing between the devices equalled five device diameters. A half-wavelength spacing was recently found to be optimal by a numerical study [7], though without a clear explanation, and also appears similar to spacings proposed by wave-power developers.

Both the parallel-to-crests and the perpendicular-to-crests orientations of a pair of devices achieved significantly higher amplitudes than the single device, reaching factors of 2.53 ± 0.02 and 2.51 ± 0.02 times the incident wave amplitude for the parallel and perpendicular orientations respectively, compared with the maximum of 1.97 ± 0.04 for the single device. Since this gain in amplitude is about 25 %, the power per device removed from the incident waves can be increased by roughly 50 % by appropriate grouping of devices into an array.

The parallel orientation achieved a significant reduction in resonant frequency, from about $\omega/\omega_0 = 0.96$ to $\omega/\omega_0 = 0.92$. Therefore, devices in this parallel orientation could be about 8 % smaller in their vertical dimension as well as deliver the enhanced power just-noted. Meanwhile, the resonant frequency for the perpendicular orientation was unchanged from the single-device value of $\omega/\omega_0 = 0.96$.

Amplitudes for the parallel orientation fell off rapidly as fre-
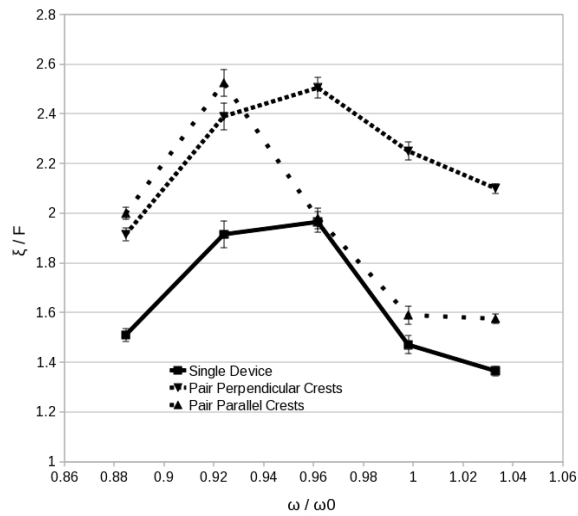
Figure 3: Peak displacements $\hat{\xi}$ scaled by incident wave amplitude F, as a function of incident wave frequency ω scaled by single-device linear inviscid natural frequency ω_0 given by (5). Solid line: single WEC device; Sparse-dotted line: a pair of devices parallel to wave crests; Closely-dotted line: a pair perpendicular to wave crests. Error bars show 95 % statistical confidence limits.

quency increased from the resonant value, dropping almost to the single-device values. A sharper peak implies a reduction in damping, making a pair of parallel devices more sensitive to shifts in the incident wave frequency. This is consistent with the qualitative prediction of (3). Meanwhile the perpendicular orientation exhibited a broader peak, consistently with (4), implying increased damping and thus greater tolerance to the wave climate.

As with the single device, tests were undertaken to assess the importance of reflection versus resonance; by sealing the bottom of one of the cylinders, a non-resonating device was created. For the parallel orientation, C6 was sealed; for the perpendicular orientation, B5 was sealed. The tests were run at $L = 0.065$ mm, i.e. $\omega/\omega_0 = 0.96$. For the parallel orientation, the results (a scaled amplitude of 1.98 ± 0.02) were statistically indistinguishable at 95% confidence. However, for the perpendicular orientation, the amplitude in the resonating device when the other device was made non-resonating fell significantly, from 2.51 ± 0.02 to 2.00, and thus was statistically indistinguishable from a single resonating device.

This implies that the parallel orientation delivered its benefit via a surface-wave reflection mechanism, despite the device size being less than 1/10 of the wavelength. Conversely, the perpendicular orientation delivered its benefit via a coupled eigenmode mechanism.

Conclusion

Laboratory experiments showed that appropriate arrangement of a pair of model wave-energy converter devices significantly enhanced the power extracted from waves. The power per device extracted from the waves and potentially available for electricity generation could be increased by roughly 50 % when devices were paired a half-wavelength apart. An enhancement had been predicted theoretically in the literature, but not demonstrated experimentally.

A similar increase in power was achieved by devices oriented both parallel and perpendicular to the wave crests. However, significant differences in frequency response and in the underlying coupling mechanism were found between the parallel and perpendicular orientations. Parallel orientation resulted in a lower resonant frequency and a sharper resonant peak, implying that somewhat smaller and thus cheaper machines could deliver the same power, but also that the pair would be more sensitive to changes in incident wave frequency. Perpendicular orientation did not significantly shift resonant frequency, but delivered the enhanced power with a broader resonant peak, implying tolerance to changes in incident wave frequency.

Finally, it should be re-iterated that the present results are preliminary and should be both repeated in a large wave basin under turbulent conditions, and undertaken for larger numbers of devices, as well as devices operating in different modes.

References

[1] Falcão, A. F. O. (2010). Wave energy utilization: A review of the technologies. *Renewable & Sustainable Energy Rev.*, 14:899–918.

[2] Evans, V. D.(1982). Wave-power absorption by systems of oscillating surface pressure distributions. *J. Fluid Mech.*, 114:481-499.

[3] Simon, M. J. (1982). Multiple scattering in arrays of wave-energy devices. Part 1. A matrix method using a plane-wave approximation. *J. Fluid Mech.*, 120: 1-25.

[4] Falnes, J., Budal, K. (1982). Wave-power absorption by parallel rows of interacting oscillating bodies. *Applied Ocean Res.*, 4(4), 194-207.

[5] Falnes, J., McIver, P. (1985). Surface wave interactions with systems of oscillating bodies and pressure distributions. *Applied Ocean Res.*, 7(4), 225-234.

[6] Mei, C. (2012). Hydrodynamic principles of wave power extraction. *Phil. Trans. R. Soc. A*, 370: 208-234.

[7] de Andrés, A. D., Guanche, R., Meneses, L. , Vidal, C., Losada, I. (2014). Factors that influence array layout on wave energy farms. *Ocean Eng.*, 82: 32-41.

[8] Olvera, A. Prado, E. and Czitrom, S. (2007). Parametric resonance in an oscillating water column. *J. Eng. Math.*, 57:1-21.

[9] Illesinghe, S. and Hasan, M. K., Manasseh, R. (2012) Multiphase dynamics of oscillating-water-column ocean wave energy converters. *18th Australasian Fluid Mechanics Conference, Launceston, Australia, 3-7 December 2012*, paper 371.

[10] Hino, M., Sawamoto, M., Takasu S. (1976). Experiments on transition to turbulence in an oscillatory pipe flow. *J. Fluid Mech.*, 75(2),193-207.

[11] Hasan, M. K., Manasseh, R. (2014) Dissipation in oscillating water columns. *19th Australasian Fluid Mechanics Conference, Melbourne, Australia, 8-11 December 2014*.

[12] Manasseh, R., Ooi, A. (2009). Frequencies of acoustically interacting bubbles. *Bubble Sci., Eng. & Tech.*, 1(1-2), 58-74.

[13] Kulpe, J. A., Leamy, M. J., Sabra, K. G. (2013). Modeling the acoustic scattering from large fish schools using the Bloch-Floquet theorem. *J. Acous. Soc. Am.*, 133(5), 3538.